Upper and Lower Bounds on the Drag Coefficient of a Sphere in a Power-Model Fluid

MELVIN L. WASSERMAN and JOHN C. SLATTERY

Northwestern University, Evanston, Illinois

The equation of continuity and the stress equations of motion are not sufficient in themselves to describe the motion of matter under given boundary conditions. In addition one must describe the behavior of the particular material to be considered by stating the relation between stress and deformation, the constitutive equation. A number of properly invariant constitutive equations have been proposed. Reiner (*17*) and Rivlin (*18, 19;* see also *21*) present the most general isotropic relation between stress and rate-of-deformation for homogeneous material. Oldroyd (*13, 14*) gives an excellent discussion of the formulation of properly invariant constitutive equations; he examines in detail the simplest constitutive equations which reduce to experimentally observed viscoelastic behavior at small rates of strain. Rivlin and Ericksen (*20*) assume the stress to be a function of the gradients of velocity, acceleration, second acceleration, Noll (*12, 5*) and Green and Rivlin (*6, 7*) consider memory effects; that is, the state of stress in the fluid is assumed to depend upon its past history as well as its current kinematic state. All of these proposals appear to be qualitatively consistent with observed viscometric flows (for example, flow in a cone-plate viscometer, flow between rotating concentric cylinders, flow through a circular cylindrical tube) for some materials with the exception that the Stokesian fluid model proposed by Reiner and by Rivlin does not properly predict observed normal stresses (*11*).

The Stokesian fluid model for an incompressible fluid*

$$t^i_j = -p\delta^i_j + \beta d^i_j + \gamma d^i_k d^k_j \tag{1}$$

$$\beta = \beta(II, III),\ \gamma = \gamma(II, III) \tag{2}$$

$$II = d^i_i d^j_i,\ III = det(d^i_j) \tag{3}$$

$$d_{ij} = (v_{i,j} + v_{j,i})/2 \tag{4}$$

is by far the simplest of all the constitutive equations proposed. It includes as special cases the simple empirical models long used in engineering work to represent the results of viscometric experiments such as the power model

$$\tau^i_j = t^i_j + p\delta^i_j = 2m(2II)^{(n-1)/2} d^i_j \tag{5}$$

While the power model cannot fully represent the behavior of any real fluid presently known (an immediate objection is that it does not predict nonzero and finite limiting viscosities at very low and at very high rates of deformation), over a limited range of stress it often gives a satisfactory approximation for the stress vs. rate-of-deformation curve from a viscometric study [or in terms of Noll's theory for simple fluids, it gives a satisfactory approximation for the first material function in a viscometric flow (*5*)]. In practice engineers have been using the power model [also the Ellis model (*22*), the Sisko model (*23*), and many others] as an approximate description for the behavior of real fluids which on the basis of viscometer studies appear to be approximately power-model fluids over a limited range of stress, but which probably exhibit normal stress effects (*11*) (and according to popular usage would be called *viscoelastic**). It seems reasonable to ask about the error incurred in using this model to represent the behavior of such a fluid in a more complicated geometry, where according to Noll's theory it is entirely possible that a description based upon viscometric measurements would be meaningless. One may be certain that an analysis based upon such a simple model could not describe the velocity and pressure fields in all details, but one might expect a reasonable prediction for a gross effect, for example the drag coefficient in flow past a sphere. In an attempt to gain a partial answer to this question, in what follows variational methods are used to develop upper and lower bounds for the drag coefficient for a sphere moving slowly through a power-model fluid; the results are compared with available experimental data (*22, 23*).

PREVIOUS WORK

Leslie (*10*) considered small perturbations from the static case to obtain an approximate solution for creeping flow past a sphere of a fluid described by the five-constant Oldroyd model (*14*). Caswell and Schwarz (*4*) investigated creeping flow past a sphere of a Rivlin-Ericksen fluid; following Proudman and Pearson (*16*), they obtained a uniform approximation to the stream function by matching Stokes expansions, satisfying the no-slip condition at the surface of the body, to Oseen expansions satisfying the boundary condition at infinity. Tomita (*24*) obtained an upper bound to the drag coefficient for a sphere moving slowly through a power-model fluid by assuming a stream function which satisfied the necessary boundary conditions (the variational approach developed in his paper was not used); errors in his series computations have been pointed out and corrected (*22, 25*), and his numerical integrations have been refined (*25*). Recently somewhat better upper bounds than those of Tomita have been calculated by means of a variational principle (*23*). Ziegenhagen, Bird, and Johnson (*26*) have also used this variational principle for upper bounds to the drag coefficient in a fluid described by a very simple two-constant model.

Unfortunately there are no data presently available with which to compare the calculations of Leslie and of Caswell and Schwarz. The only data possibly suitable for comparison with calculations for the power model (the limitations of the

* Comma notation stands for covariant differentiation, and the summation convention is employed throughout. In Cartesian, orthogonal coordinates there is no distinction between the covariant and contravariant components of a tensor, and the comma denotes partial differentiation with respect to the space coordinate whose index follows. For the equations of continuity and of motion in spherical coordinates see for example reference 2, pp. 83 to 91.

* The term "viscoelastic" does not appear to have a precise meaning except in the linearized theories. Coleman and Noll (*5*) use the word to refer to materials which do not obey the classical laws of fluid mechanics or elasticity.

power model are discussed in the beginning of the paper) are for five aqueous solutions of carboxymethylcellulose (22, 23). These data are shown in Figure 2 in comparison with previous theoretical results and the calculations described below.

VARIATIONAL THEOREMS

Because the variational theorems used here have been developed previously (*15, 1, 8, 9*), the results are stated here without proof.

Velocity variational theorem

A particular situation is considered.

1. The fluid is incompressible:

$$v^i_{,i} = 0 \tag{6}$$

2. The flow is independent of time.

3. The inertial terms in the equation of motion are negligibly small or identically zero:

$$v^i v^j_{,i} = 0 \tag{7}$$

4. The constitutive equation can be represented in the form:

$$\tau^i_j = t^i_j + p\delta^i_j = \partial\Gamma/\partial d^j_i \tag{8}$$

5. The external body force per unit mass f_i may be represented by a single-valued potential (that is, the acceleration of gravity).

$$f_i = -\varphi_{,i} \tag{9}$$

Under the above restrictions Pawlowski (*15*), Bird (*1*) and Johnson (*8, 9*) have shown that for a generalized Newtonian fluid [a special case of the Stokesian fluid, Equation (1)]

$$t^i_j = -p\delta^i_j + 2\eta d^i_j, \quad \eta = \eta(II) \tag{10}$$

the functional J_v

$$J_v = \int_{\bar{V}} \Gamma \, d\bar{V} \tag{11}$$

$$\Gamma = \Gamma(v^i) = \int_0^{II} \eta \, dII \tag{12}$$

assumes stationary values for velocity trial functions satisfying the following admissibility conditions:

1. Equation (6) is satisfied by the trial function.
2. The velocity trial function satisfies a known velocity distribution on all bounding surfaces of the system.

Johnson (9) has shown further that if the fluid is dilatant ($\eta > 0$, $\partial\eta/\partial II > 0$), J_v assumes a minimum value for the correct solution to the equations of motion. If the fluid is pseudoplastic ($\eta > 0$, $\partial\eta/\partial II < 0$), J_v is also minimized provided that

$$\eta + 2\frac{\partial\eta}{\partial II} II > 0 \tag{13}$$

For a power-model fluid

$$\eta = m(2II)^{(n-1)/2} \tag{14}$$

$$\Gamma = \frac{m}{n+1}(2II)^{(n+1)/2} \tag{15}$$

which means that the velocity variational principle is a minimum principle for $n > 0$.

Stress (or Reciprocal) Variational Theorem

The same restricted physical situation considered in 1 through 5 of the preceding section is again considered, but is modified so that 4 reads

$$4'\ d_{ij} = \partial\bar{\Gamma}/\partial\tau^{ij} \tag{16}$$

Johnson (*8, 9*) shows that for a generalized Newtonian fluid the functional H_τ

$$H_\tau = -\int_V \bar{\Gamma} \, dV - \int_{S_v} \psi_v \, dS \tag{17}$$

$$\bar{\Gamma} = \bar{\Gamma}(\tau_{ij}) = \int_0^{II_\tau} \frac{dII_\tau}{4\eta(II_\tau)} \tag{18}$$

assumes stationary values. The function ψ_v is defined by the boundary condition that on that portion of the bounding surfaces S_v on which velocity is specified

$$S_v: \quad v_i + \frac{\partial\psi_v}{\partial(t^{ij}n_j)} = 0 \tag{19}$$

There are three admissibility conditions which the stress trial function used in Equation (17) must satisfy.

1. $$\tau^{ij}_{,j} - p^{,i} + \rho f^i = 0 \tag{20}$$

2. $$S_t: \quad \tau^{ij}n_j - pn^i + \psi_t{}^{*i} = 0 \tag{21}$$

3. $$S_v: \quad t^{ij}n_j = \tau^{ij}n_j - pn^i \tag{22}$$

Here S_t is that portion of the bounding surface of the system on which stress is specified; $\psi_t{}^{*i}$ is some known vector function of position on the S_t surface.

For a power-model fluid, since

$$II_\tau = 2m^2 \ (2II)^n \tag{23}$$

then

$$\eta = m\left[\frac{II_\tau}{2m^2}\right]^{(n-1)/2n} \tag{24}$$

$$\bar{\Gamma} = \frac{n\, m^{-1/n}}{n+1}\left[\frac{1}{2}II_\tau\right]^{(1+n)/2n} \tag{25}$$

It has been shown that the stress variational theorem is a maximum principle under the same conditions that the velocity principle is a minimum (8, 9).

Relation Between Velocity and Stress Variational Theorems

If the boundary value problem has a unique solution and if conditions are met which ensure that the velocity principle is a minimum principle and that the stress principle is a maximum principle, then (8)

$$H_\tau \leq J \leq J_v \tag{26}$$

The quantities H_τ and J_v are evaluated using any admissible trial functions in Equations (11) and (17).

UPPER AND LOWER BOUNDS FOR THE DRAG COEFFICIENT

For the steady state, creeping flow past a sphere of an infinite body of incompressible fluid, the macroscopic momentum balance (2) may be combined with the macroscopic energy balance (2) to obtain

$$VF = \int_{\bar{V}} \tau^{ij}d_{ij} \, d\bar{V} \tag{27}$$

This reduces for a generalized Newtonian fluid, Equation (10), to

$$VF = \int_{\bar{V}} 2\eta II \, d\bar{V} \tag{28}$$

It is more convenient to speak in terms of the drag coefficient (or friction factor) f

$$f = 8F/(\rho V^2 \pi D^2) \tag{29}$$

From Equations (29), (28), and (14) one has for a power-model fluid

$$f = 24X/N_{Rm} \tag{30}$$

$$X = \frac{2^{n-1}}{3} \int_0^{\pi} \int_0^1 (2II^*)^{(n+1)/2}\, x^{-2} \sin\theta \, dx \, d\theta \tag{31}$$

$$II^* = \left[\frac{D}{2V}\right]^2 II \tag{32}$$

$$N_{Rm} = \rho V^{2-n} D^n/m \tag{33}$$

Comparison of Equations (31) and (11) shows that for a power-model fluid J_v is proportional to X

$$J_v = \alpha X, \quad \alpha = 3\pi m V^{n+1} D^{2-n}/(n+1) \tag{34}$$

From Equation (26) one sees that J_v/α is an upper bound to X and H_τ/α a lower bound; J_v and H_τ hereafter indicate the quantities calculated using any admissable trial functions in Equations (11) and (17). In the sections to follow velocity and stress trial functions are assumed so that these upper and lower bounds may be obtained.

CALCULATIONS FOR UPPER BOUND

The details of the physical situation are that there is a sphere of diameter D fixed at the center of a spherical coordinate system (θ measured from the positive z axis) with the fluid very far away from the sphere moving in the positive z direction with a velocity V. Noting symmetry, it is assumed that

$$v_\phi = 0, \quad v_r = v_r(r,\theta), \quad v_\theta = v_\theta(r,\theta) \tag{35}$$

As discussed previously, the trial functions for the two components of velocity must be chosen to satisfy continuity and the boundary conditions on velocity:

$$r = D/2: \quad v_r = v_\theta = 0 \tag{36}$$

$$r \to \infty: \quad v_z \to V \tag{37}$$

Continuity is satisfied by writing the velocity components in terms of the stream function:

$$v_r = -\frac{1}{r^2 \sin\theta} \frac{\partial\psi}{\partial\theta}, \qquad v_\theta = \frac{1}{r\sin\theta} \frac{\partial\psi}{\partial r} \tag{38}$$

[In terms of the stream function Equation (37) becomes $r \to \infty$: $\psi \to -(Vr^2 \sin^2\theta)/2$.] The trial function for ψ is taken to be

$$\psi = -\frac{1}{2} V r^2 \sin^2\theta \,[1-(D/2r)^\sigma]^2 \tag{39}$$

which satisfies the boundary conditions of Equations (36) and (37). This was suggested by the assumed stream function of Tomita (*24*); in contrast with his it has one undetermined parameter σ.

Substituting Equation (39) into Equation (31), one obtains

$$X = 2^n\, 3^{(n-1)/2}\, \sigma^{n+1} \int_0^{\pi} \int_0^1 x^{(\sigma+1)(n+1)-4}\, U^{(n+1)/2} \sin\theta \, dx \, d\theta \tag{40}$$

$$U = (1-x^\sigma)^2 \cos^2\theta + \frac{1}{12}[(\sigma-1) - (2\sigma-1)x^\sigma]^2 \sin^2\theta \tag{41}$$

As discussed in the preceding section, X must be minimized to determine the optimum value of σ. The function X was evaluated with an IBM-709 by means of a two-dimensional Simpson's rule quadrature for various values of n. The value of σ needed to carry out this numerical integration was estimated by expanding $A^{(n+1)/2}$ in Equation (40) in a binomial series about 1.0 and solving the equation $\partial X/\partial\sigma = 0$ by the Newton-Raphson method. The binomial series approach does not give accurate values of X, but it does appear to give good estimates for σ; values of σ slightly smaller and larger than the value obtained from the series approach were used for some values of n and in all cases X either increased or remained stationary.

The error in the Simpson's rule calculation is estimated to be less than 0.1%. The value of X for $n = 1.0$ is 1.006 if evaluated analytically; the computed value is 1.005. In a few cases the numbers of panels in both the x and θ directions were doubled with no resultant change in X to four significant figures.

CALCULATIONS FOR LOWER BOUND

Admissible stress trial functions must satisfy the stress equations of motion, Equations (20). By analogy with Stokes' solution and with the work in the proceding section, one may assume that there are only four nonzero components of the stress tensor in spherical coordinates. The two stress equations of motion in spherical coordinates not identically satisfied are (in terms of the physical components of the stress tensor)

$$\frac{\partial(p+\varphi\rho)}{\partial r} = \frac{1}{r^2}\frac{\partial}{\partial r}(r^2\tau_{rr}) + \frac{1}{r\sin\theta}\frac{\partial}{\partial\theta}(\tau_{r\theta}\sin\theta) - (\tau_{\phi\phi}+\tau_{\theta\theta})/r \tag{42}$$

$$\frac{\partial(p+\rho\varphi)}{\partial\theta} = \frac{1}{r}\frac{\partial}{\partial r}(r^2\tau_{r\theta}) + \frac{1}{\sin\theta}\frac{\partial}{\partial\theta}(\tau_{\theta\theta}\sin\theta) + \tau_{r\theta} - \tau_{\phi\phi}\cot\theta \tag{43}$$

Since the only external force is due to gravity, it is represented by a potential according to Equation (9). The variables p and φ may be eliminated by equating

$$\partial(p+\rho\varphi)/\partial r\partial\theta = \partial(p+\rho\varphi)/\partial\theta\partial r \tag{44}$$

The trial stress distribution is taken to be

$$\tau_{r\theta} = -A\,x^B \sin\theta\, m(2V/D)^n \tag{45}$$

$$\tau_{rr} = -(Cx^D + C'x^B)\cos\theta\, m(2V/D)^n \tag{46}$$

$$\tau_{\theta\theta} = -(Fx^D + F'x^B)\cos\theta\, m(2V/D)^n \tag{47}$$

$$\tau_{\phi\phi} = -(Ex^D + E'x^B)\cos\theta\, m(2V/D)^n \tag{48}$$

After substituting Equations (45) to (48) into Equation (44) and after equating the coefficients of $[x^D\cos^2\theta/(r\sin\theta)]$, $[x^B\cos^2\theta/(r\sin\theta)]$, $[x^D\sin\theta/r]$ and $[x^B\sin\theta/r]$ each to zero, we obtain, respectively

$$E = F, \quad E' = F', \quad D = 2 \tag{49 to 51}$$

$$AB^2 - B(3A + C' - F') + 2(A + C' - F') = 0 \tag{52}$$

It is arbitrarily assumed that

$$B = 4, \quad C' = -C, \quad F' = -F \tag{53 to 55}$$

to obtain from Equation (52)

$$C' = 3A + F' \tag{56}$$

The stress trial functions are now functions of only two undetermined coefficients A and F'. Admissibility condition Equation (21) does not apply because there are no stress boundary conditions; Equation (22) serves as a definition for the stress t^{ij} in terms of p and τ^{ij}.

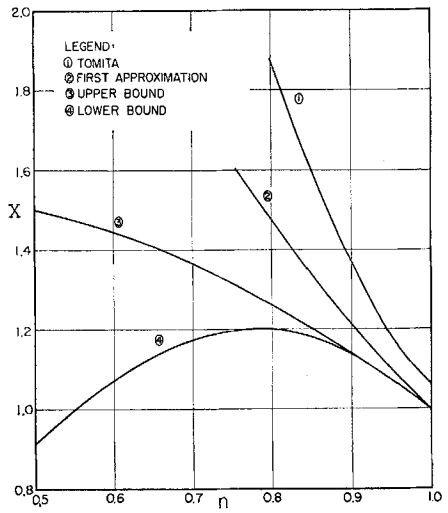

Fig. 1. Comparison of the upper and lower bounds on X as given in Table 1 with a previously reported first approximation (23) and with the corrected numerical integrations (25) from Tomita's calculations (24).

Boundary condition Equation (19) suggests that in Equation (17) one may take

$$\psi_v = -\, v_i n_j f^{ij} \tag{57}$$

The bounding surfaces of the system are the sphere and a sphere of infinitely large radius. On the former, ψ_v is identically zero because of the boundary conditions of Equation (36); on the latter

$$\psi_v = pv_r - (v_r\ \tau_{rr} + v_\theta\ \tau_{r\theta}) \tag{58}$$

where the pressure p may be determined from Equations (42) to (43) to be (within an additive constant)

$$p = [-\,(A + F')x^4\ \cos\theta + F'\ x^2\ \cos\theta]\, m(2V/D)^n \tag{59}$$

Substitution of the above results into Equation (17) gives

$$H_\tau = m\ (D/2)^{2-n}\, V^{n+1}\, 2\pi \left[\frac{-\,n}{n+1} Y + 2A\right] \tag{60}$$

where

$$Y = \int_0^\pi \int_0^1 \left[A^2 x^8 \sin^2\theta + \frac{3}{2}(3A^2 + 2AF' + F'^2)\ (x^2 - x^4)^2 \cos^2\theta \right]^{(n+1)/2n} x^{-4} \sin\theta\, dx\, d\theta \tag{61}$$

The constants A and F' are chosen to make H_τ a maximum; they are found to be

$$A = -\,F' = (2/I)^n \tag{62}$$

$$I = I(n) = \int_0^\pi \int_0^1 [x^8 \sin^2\theta + 3(x^2 - x^4)^2 \cos^2\theta]^{(n+1)/2n}\, x^{-4} \sin\theta\, dx\, d\theta \tag{63}$$

Putting these results back into Equation (60) and referring to the previous section on upper and lower bounds for the drag coefficient, one may obtain the final expression for the lower bound on the drag coefficient as

$$X_{\text{lower}} = 2^{2n} I^{-n}/3 \tag{64}$$

As a check, for $n = 1$

$$I = 4/3, \quad A = 3/2, \quad F' = -\,3/2$$

which agrees with Stokes' solution.

TABLE 1. UPPER AND LOWER BOUNDS OF X

n	Upper bound	σ [Equation (39)]	Lower bound
1.000	1.005	1.141	1.006
0.950	1.073	1.210	1.082
0.900	1.140	1.300	1.141
0.891	1.151	1.332	1.150
0.873	1.174	1.368	1.165
0.850	1.201	1.415	1.180
0.800	1.260	1.526	1.199
0.763	1.303	1.621	1.198
0.750	—	—	1.196
0.748	1.318	1.655	1.196
0.700	1.366	1.771	1.173
0.600	1.445	1.998	1.072
0.500	1.499	2.172	0.9165
0.400	1.549	2.315	0.7280
0.300	1.617	2.432	0.5278
0.200	1.704	2.582	0.3326

TABLE 2. COMPARISON WITH EXPERIMENTAL DATA (22, 23)

Solution	n	m	ρ	$X_{\text{avg.}}$	Avg. % error* in $X_{\text{avg.}}$	No. of pts.† compared
0.6% CMC (high)	0.700	3.88	0.9986	1.270	28.7	12
1.5% CMC (medium)	0.891	1.56	1.0026	1.146	2.6	5
2.5% CMC (medium)	0.763	12.0	1.007	1.250	12.9	21
4.0% CMC (low)	0.873	2.09	1.0140	1.170	12.6	6
5.0% CMC (low)	0.748	9.11	1.0190	1.257	66.0	21

* The average percentage of error is positive with the exception of five points for the 2.5% (CMC) system and four points for the 1.5% CMC system.
2.5% CMC 5 pts.: −1.8% error, 16 pts.: +16.4% error
1.5% CMC 4 pts.: −2.7% error, 1 pt.: +2.1% error
The average percentage of error is obtained by summing the absolute values of the errors of the individual points and dividing by the number of points.
† Fewer points appear on Figure 2 because of overlapping.

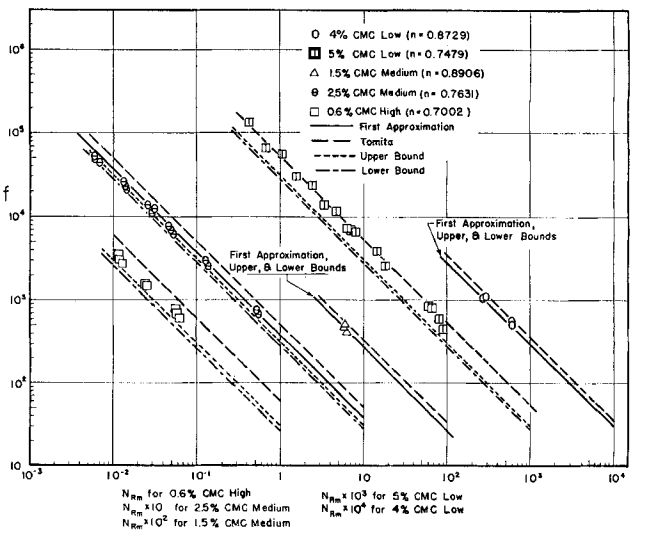

Fig. 2. Comparison of available experimental data for the drag coefficient (22, 23) with a previously reported first approximation (23), with the corrected numerical integrations (25) from Tomita's calculations (24), and with the upper and lower bounds from Table 1.

The function I was computed by a two-dimensional Simpson's rule quadrature. Doubling the number of panels in each direction for a few values of n less than one did not change the value (to four significant figures) The function X for $n = 1$ was computed to be 1.006, which is 0.6% above the analytical value. It is believed therefore that 1% is a conservative estimate of the computational error for values of n less than unity.

COMPARISON WITH OTHER WORK

In Figure 1 are plotted previously determined upper bounds to the function X defined in Equation (30) (*23, 24*). The plot due to Tomita (*24*) represents recently corrected numerical integrations (*25*). The upper bound found here is considerably below both of these.

In Table 2 the averages of the upper and lower bounds to X as given in Table 1 and Figure 1 are compared with the available experimental data (*22, 23*); a point-by-point comparison is shown in Figure 2 as well. Approximation of capillary viscometer data for these fluids by the power model appears to be satisfactory over the range of stress estimated to be important in the sphere experiments*; a detailed discussion is given elsewhere (*23*). Only sphere data with $N_{Rm} < 0.1$† and with the Newtonian correction for wall effects (3) less than 3% were used. Agreement between the experimental and theoretical results is not very encouraging. This may be an indication either that the approximation by the power model of the stress vs. rate-of-deformation curve obtained from the capillary viscometer data was not sufficiently precise or that even for a gross calculation such as the prediction of the drag coefficient, a rheological model based upon viscometric data is not satisfactory for these fluids. Noll's theory of simple fluids (*12, 5*) suggests this latter possibility. The accuracy of the experimental data is examined elsewhere (*22*).

CONCLUSIONS

1. Upper and lower bounds to the drag coefficient on a sphere moving slowly through a power-model fluid have been obtained by variational methods. The upper bound is considerably below those previously published; a lower bound has not been given before.

2. Available experimental data are compared with the average of the upper and lower bounds. The poor agreement may indicate that simple rheological models are not useful approximations to the behaviors of these fluids. Additional experimental data are necessary to clarify the situation.

NOTATION

$A, B, C, E, F, B', C', E', F'$ = parameters in stress trial functions, Equations (45) to (48)
d_{ij} = rate-of-deformation tensor, Equation (4)
D = diameter of the sphere
f = drag coefficient for sphere, Equation (29)
f_i = external body force vector
F = force which the fluid exerts on the sphere in the positive Z direction
H_τ = stress variational functional, Equation (17)
I = function defined by Equation (63)
J = value of J_v corresponding to the exact solution of the problem
J_v = velocity variational functional, Equation (11)
m, n = constants in the power model, Equation (5)
n_j = outwardly directed unit vector normal to bounding surface of the system
N_{Rm} = modified Reynolds number, Equation (33)
p = pressure
r = radial spherical coordinate
S_t = portion of bounding surface of the system on which stress is specified
S_v = portion of bounding surface of the system on which velocity is specified
t_{ij} = stress tensor
U = factor in Equation (40), defined by Equation (41)
v_i = velocity vector
v_r, v_θ, v_ϕ = physical components of velocity vector in spherical coordinates
V = velocity of fluid at distance from the sphere in positive Z direction
$\overline{V}$ = volume of system
x = dimensionless radial spherical coordinate, $D/2r$
X = factor defined by Equation (30)
Y = function defined by Equation (61)
II, III = invariants of the rate-of-deformation tensor, Equation (3)
II_τ, III_τ = invariants of the stress tensor, definitions parallel to those in Equation (3)
II^* = dimensionless form of II, Equation (32)

Greek Letters

α = factor defined by Equation (34)
β, γ = functions in Stokesian fluid model, Equation (1)
Γ = potential for stress tensor, Equation (8)
$\overline{\Gamma}$ = potential for rate-of-deformation tensor, Equation (16)
δ^i_j = Kronecker delta
η = apparent viscosity in generalized Newtonian fluid model, Equation (10)
Θ, ϕ = spherical coordinates; Θ measured from positive Z axis
ρ = density
σ = parameter in trial function for ψ, Equation (39)
$\tau_{rr}, \tau_{\theta\theta}, \tau_{\phi\phi}, \tau_{r\theta}$ = physical components of τ_{ij} in spherical coordinates
τ_{ij} = viscous portion of the stress tensor, Equation (5)
φ = potential for external body force vector, Equation (9)
ψ = stream function, Equation (38)
ψ^{*i}_t = known vector function of position on S_t, Equation (21)
ψ_v = potential for velocity boundary condition, Equation (19)

LITERATURE CITED

1. Bird, R. B., *Phys. Fluids*, 3, 539 (1960).
2. ———, W. E. Stewart, and E. N. Lightfoot, "Transport Phenomena," Wiley, New York (1960).
3. Brenner, Howard, *Chem. Eng. Sci.*, 16, 242 (1961).
4. Caswell, B., and W. H. Schwarz, *J. Fluid Mech.*, 13, 417 (1962).
5. Coleman, B. D., and Walter Noll, *Ann. N. Y. Acad. Sci.*, 89, 672 (1961).
6. Green, A. E., and R. S. Rivlin, *Arch. Rational Mech. Anal.*, 1, 1 (1957).
7. *Ibid.*, 4, 387 (1960).
8. Johnson, M. W., Jr., *Phys. Fluids*, 3, 871 (1960).
9. ———, *Trans. Soc. Rheol.*, 5, 9 (1961).
10. Leslie, F. M., *Quart. J. Mech. Appl. Math.*, 14, 36 (1961).
11. Markovitz, Hershel, *Trans. Soc. Rheol.*, 1, 37 (1957).
12. Noll, Walter, *Arch. Rational Mech. Anal.*, 2, 197 (1958).
13. Oldroyd, J. G., *Proc. Roy. Soc. Lond. Ser. A*, 200, 523 (1950).

* The ranges of $[\overline{II}_v/2]^{1/2}_{\max.\ \text{sphere}}$ for the experiments used in the comparisons given in Table 2 and Figure 2 were roughly in the centers of those presented in the fifth line of Table 1 of (*22*).

† It is not clear from the experimental data that $N_{Rm} = 0.1$ is the proper upper limit for the exclusion of inertial effects.

14. ———, *ibid.*, **245**, 278 (1958).
15. Pawlowski, J., *Kolloid Z.*, **138**, 6 (1954).
16. Proudman, Ian, and J. R. A. Pearson, *J. Fluid Mech.*, **2**, 237 (1957).
17. Reiner, Markus, *Am. J. Math.*, **67**, 350 (1945).
18. Rivlin, R. S., *Nature*, **160**, 611 (1947).
19. ———, *Proc. Roy. Soc. Lond., Ser. A*, **193**, 260 (1948).
20. ———, and J. L. Ericksen, *J. Rat. Mech. Anal.*, **4**, 323 (1955).
21. Serrin, James, "Handbuch der Physik, Band VIII/1," S. Flügge, ed., p. 231, Springer-Verlag, Berlin, Germany, (1959).
22. Slattery, J. C., and R. B. Bird, *Chem. Eng. Sci.*, **16**, 231 (1961).
23. ———, *A.I.Ch.E. Journal*, **8**, 663 (1962).
24. Tomita, Yukio, *Bull. Japan Soc. Mech. Engrs.*, **2**, 469 (1959).
25. Wallick, G. C., J. G. Savins, and D. R. Arterburn, *Phys. Fluids*, **5**, 367 (1962).
26. Ziegenhagen, A. J., R. B. Bird, and M. W. Johnson, Jr., *Trans. Soc. Rheol.*, **5**, 47 (1961).

Manuscript received April 29, 1963; revision received October 9, 1963; paper accepted October 10, 1963. Paper presented at A.I.Ch.E. Houston meeting.

Graphite Oxidation at Low Temperature

EDWARD EFFRON and H. E. HOELSCHER

The Johns Hopkins University, Baltimore, Maryland

Although carbon oxidation processes have been an integral part of our industrial economy for many years, a complete understanding of the reaction kinetics has lagged behind practical utilization. Complications arising from the properties of solid carbon and from interfering side reactions have made the study of initial oxidation steps difficult. Knowledge of the mechanism would be of interest in fuel bed design for energy generation or chemical production and design of graphite rocket nozzles, missile heat shields, or nuclear moderating materials. This paper reports results from an investigation of the primary reaction kinetics of the carbon-oxygen reaction.

Reports from carbon-oxygen reaction studies date from the middle of the nineteenth century. Although some disagreement still exists, the conclusion that there is simultaneous liberation of carbon monoxide and carbon dioxide [first advanced by Rhead and Wheeler (*17*)] has gained wide acceptance. More recent work has shown this ratio to be an exponentially increasing function of temperature (*1, 18*). Oxygen chemisorption and the formation of a surface complex appears to be prerequisite for reaction.

Recent development of sensitive analytical tools has enabled investigators to work at ever lower temperatures where results reflecting only the primary surface reactions can be obtained. Thus Gulbransen and Andrew (*8*) by suspending graphite from a precision microbalance were able to obtain measurable rates at 425°C. However product gas compositions were not obtained. Lewis, Gilliland, and Paxton (*16*) operated a graphite fluidized bed as low as 425°C. and obtained an essentially constant ratio of carbon monoxide to carbon dioxide up to the temperature where homogeneous carbon monoxide oxidation became important. Within the past year or two workers associated with the atomic energy establishments of England and France have studied nuclear graphite oxidation at temperatures approaching 400°C. (*13, 14, 15*).

Application of pore diffusion concepts developed from the field of heterogeneous catalysis has proved fruitful in reconciling discrepancies in kinetic data previously obtained. Here again low reaction rates (low temperatures) are necessary to avoid interference from diffusion effects within the porous solid. Wicke and his associates (*24, 25*) have shown that above 500° to 600°C. pore diffusion influences must be considered important. Blyholder and Eyring (*3*), working at pressures less than 100 μ, indicated that above 600°. graphite samples thicker than 0.1 mm. were affected by pore diffusion. Two recent literature surveys covering gas-carbon reactions in general are available (*2, 22*). Extensive bibliographies are presented in both. Effron (*6*) has reviewed the literature particularly pertinent to the initiation mechanism.

EXPERIMENTAL APPARATUS AND PROCEDURE

The apparatus used during the experimental program and the procedures followed are described in detail elsewhere (*6*). The oxidation studies (except for one run to be discussed later) were carried out over ¼-in. diameter graphite rods. The reactor was stainless steel, 2-in. I.D., 5½ in. long, and ⅛ in. wall thickness. The reactor was placed at the end of a 1½-in. I.D. ceramic combustion tube packed with porcelain chips to serve as a preheater. The maximum temperature available in the preheater was 1,000°C. The graphite rods were placed in the reactor with their axes normal to the flow. An aluminum paint protected all surfaces from corrosion, and the system was thoroughly insulated. Gas samples were taken at the inlet and outlet of the reactor section. Standard devices regulated gas supply as needed.

Operating conditions used throughout the study were

$$2 < N_{Re} < 6$$

Edward Effron is with Esso Research and Engineering Company, Florham Park, New Jersey

TABLE 1

Run	Graphite type*	a,† sq. m./g.	Nominal grain size	$A_{carbon} \times 10^{-8}$, mg./min. sq. m.	$\sigma_c \times 10^{-8}$	$A_{co} \times 10^{-8}$, cc./min. sq. m.	$\sigma_{co} \times 10^{-8}$	$A_{co^2} \times 10^{-8}$, cc./min. sq. m.	$\sigma_{co2} \times 10^{-8}$
GR 1	AUC P7201	0.73	0.008	17.6	1.6	4.48	0.59	28.4	2.7
GR 4	AGKSP W16	0.42	0.019	11.2	1.7	2.17	0.031	17.3	3.3
GR 5	AGSR P2712	0.86	0.016	3.32	0.25	0.64	0.069	5.60	0.43
GR 7	AGKSP P19	0.86	0.019	7.89	0.68	1.73	0.28	13.1	0.95

* The designation of the graphites follows that of the supplier, that is the National Carbon Company. All graphites had a bulk density between 1.58 and 1.68 g./cc.
† Obtained from nitrogen adsorption by Dr. B. L. Harris, Glen Arm, Maryland.